Electronic Supplementary Material (ESI) for Journal of Materials Chemistry A.

Supplementary Information

Operando Structural and Chemical Evolutions of TiS_2 in Na-ion Batteries

Cheng-Hung Lin[1], Mehmet Topsakal[2], Ke Sun[1, 3], Jianming Bai[4], Chonghang Zhao[1], Eric Dooryhee[4], Paul Northrup[5], Hong Gan[3], Deyu Lu[6], Eli Stavitski[4], Yu-chen Karen Chen-Wiegart[1, 4]*

1. Department of Materials Science and Chemical Engineering, Stony Brook University, Stony Brook, NY 11794
2. Nuclear Science and Technology Department, Brookhaven National Laboratory, Upton, NY 11973
3. Sustainable Energy Technologies Department, Brookhaven National Laboratory, Upton, NY 11973
4. National Synchrotron Light Source II, Brookhaven National Laboratory, Upton, NY 11973
5. Department of Geosciences, Stony Brook University, Stony Brook, NY, 11794
6. Center for Functional Nanomaterials, Brookhaven National Laboratory, Upton, NY 11973

E-mail:

*Yu-chen Karen Chen-Wiegart: Karen.Chen-Wiegart@stonybrook.edu

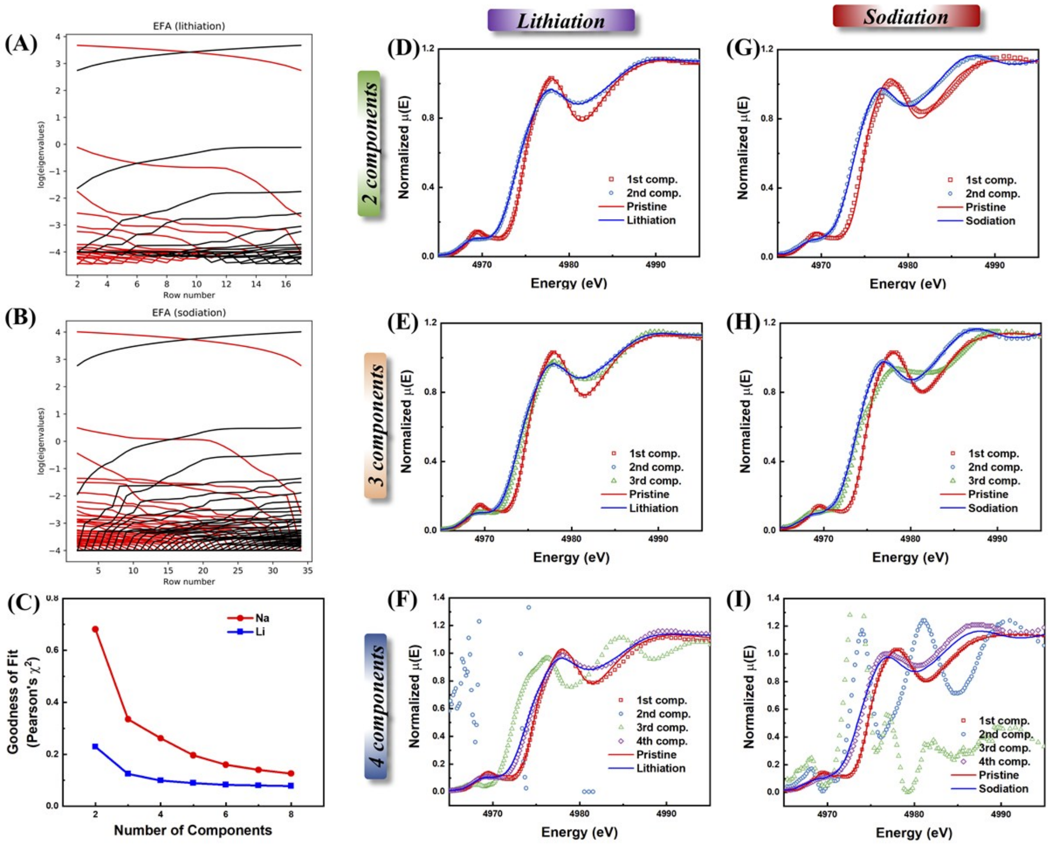

Figure S1. Evolving factor analysis (EFA) for lithiation (A) and sodiation (B) XANES spectra. Black lines denote forward EFA while the red lines denote backward EFA. Eigenvalues (in log units) are plotted as a function of the row number of the data matrix, D. (C) The goodness of fit for MCR-ALS calculation of *operando* XANES series with various number of pure components considered in the MCR-ALS method. The calculated XANES spectra of pure components derived from MCR-ALS method with various number of pure components in lithium (D-F) and sodium (G-I).

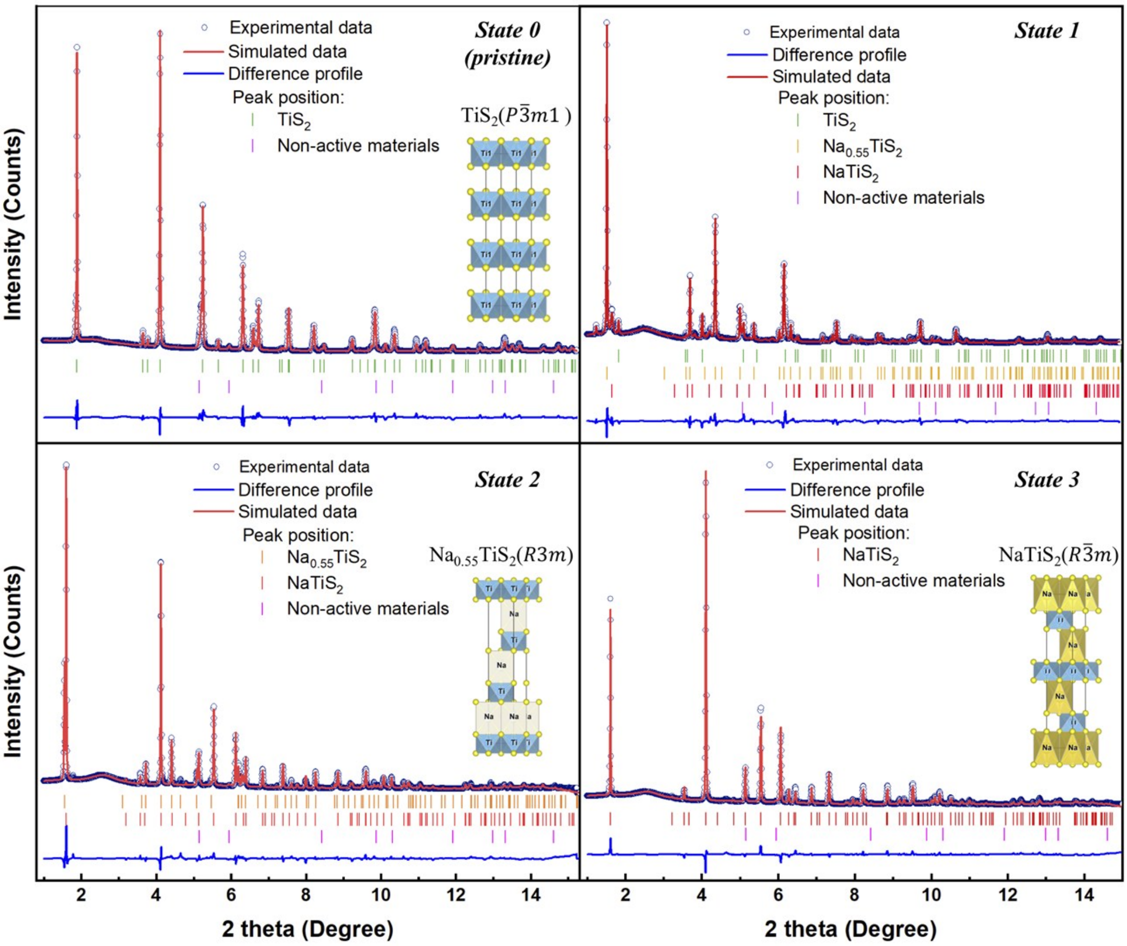

Figure S2. The individual Rietveld refinement result at different sodiated states of *ex situ* XPD patterns in Figure 5(a).

Table S1. Results of fitting parameter from Rietveld refinement and the weighted profile R-factor (R_{wp}).

	Structure	*Space group*	a, b *(Å)*	c *(Å)*	*Ratio (%)*	R_{wp} *(%)*
State 0 (Pristine)	TiS_2	$P\bar{3}m1$	*3.41*	*5.7*	*98*	*7.3*
State 1 (40% relative capacity)	TiS_2	$P\bar{3}m1$	*3.41*	*5.82*	*10*	*8.2*
	Unknown ($NaTi_3S_6$)	$P\bar{3}m1$	*3.38*	*25.83*	*7*	
	$Na_{0.55}TiS_2$	$R3m$	*3.44*	*21.02*	*62*	
	$NaTiS_2$	$R\bar{3}m$	*3.4*	*19.33*	*20*	
State 2 (82% relative capacity)	$Na_{0.55}TiS_2$	$R3m$	*3.47*	*20.83*	*23*	*11*
	$NaTiS_2$	$R\bar{3}m$	*3.51*	*20.2*	*76*	
State 3 (Full sodiation)	$NaTiS_2$	$R\bar{3}m$	*3.55*	*20.01*	*99*	*10.5*

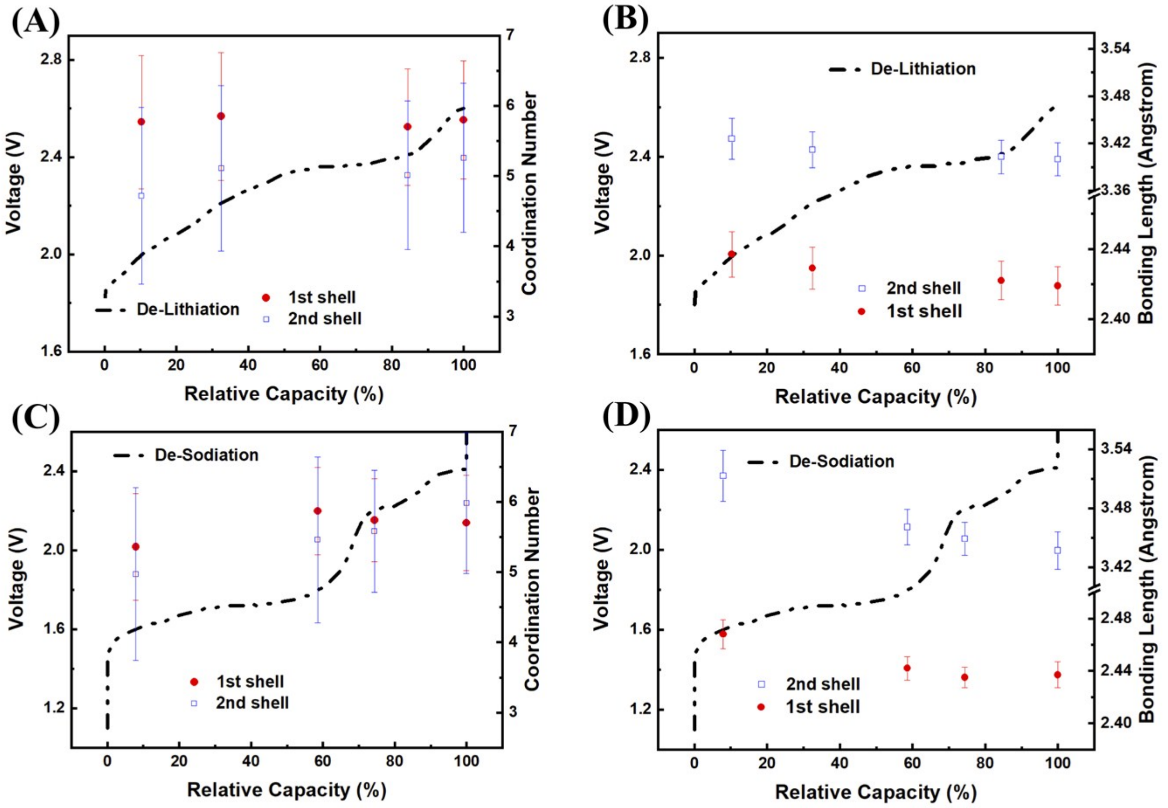

Figure S3. The modeling results of EXAFS spectra on Ti-S (1st shell) and Ti-Ti (2nd shell) in both de-lithiation/de-sodiation: (A-B) Coordination number and (C-D) bonding length evolutions.

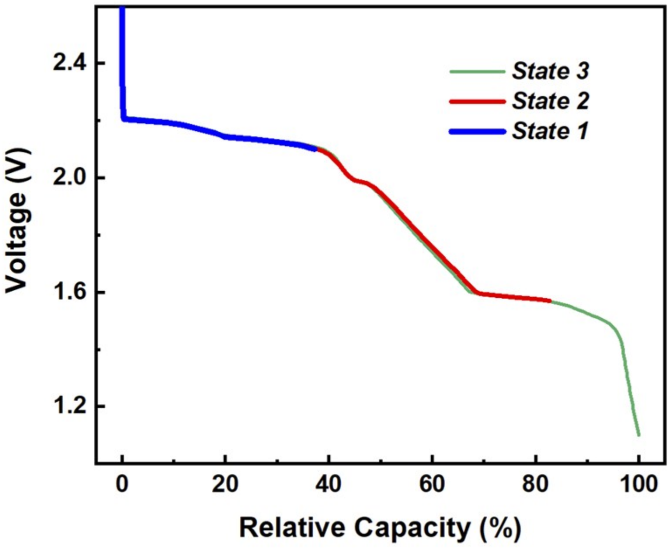

Figure S4. The electrochemical profiles of Na-TiS_2 battery at different states for *ex situ* XPD experiment.

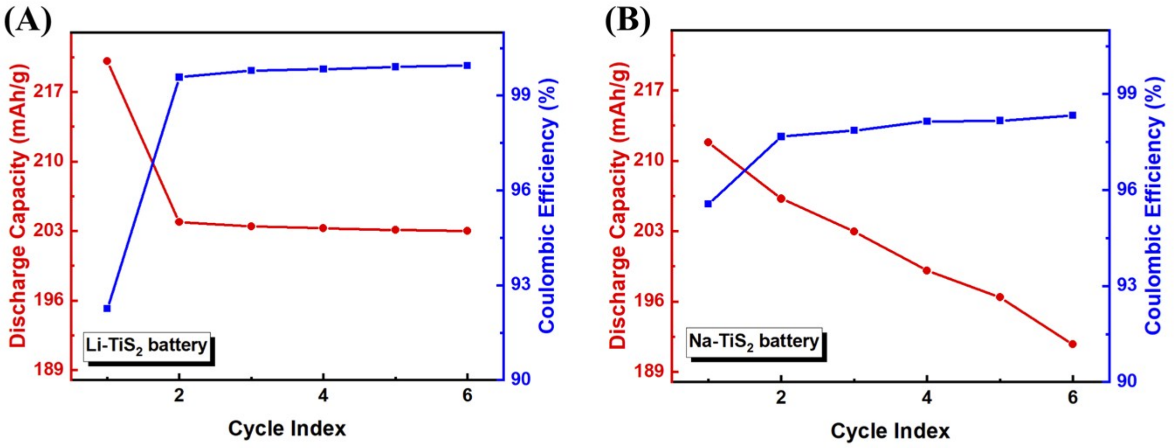

Figure S5. The discharge capacity and Coulombic efficiency as the function of cycling numbers for (A) Li-TiS_2 battery and (B) Na-TiS_2 battery.

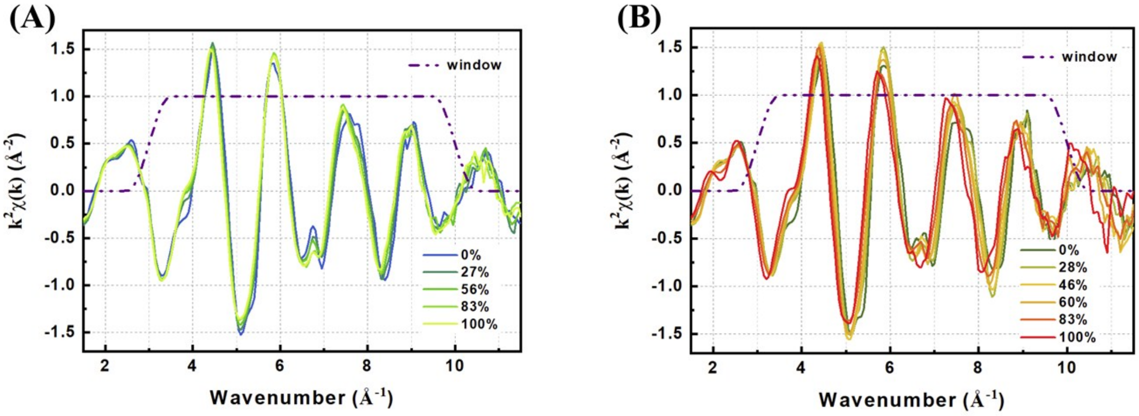

Figure S6. The corresponding k^2 - weighted EXAFS $\chi(k)$ spectra and the FT window of (A) Li-TiS_2 battery and (B) Na-TiS_2 battery.

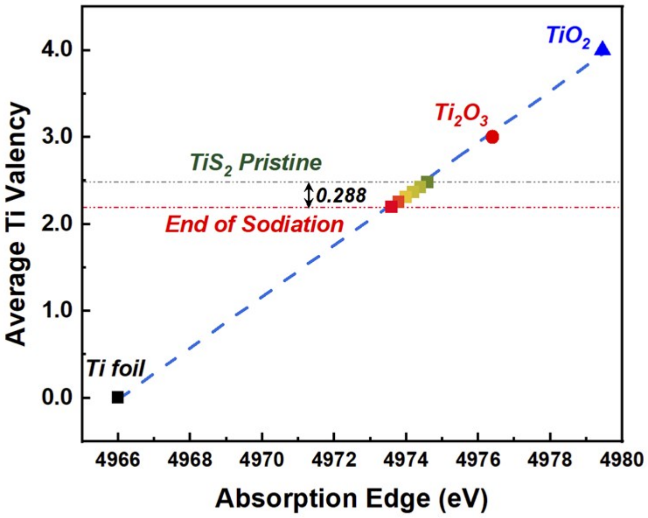

Figure S7. Fitted linear relationship of the absorption edge vs. average Ti valence state during sodiation.

On the assumption of the linear relationship between the edge position and average oxidation state, the average Ti oxidation state of TiS_2 is estimated to be ~2.5^+ rather than 4^+ because of the iono-covalent character of Ti-S bonding.[s1, s2] However, the same strategy is challenging to be applied on the S XANES spectra due to the lack of good standard spectra, which are not practical for this work to obtain pure stable intermediate or end-state electrochemical compounds. Furthermore, the more complex electronic structure among various sulfur compounds may not follow the linear relationship between the edge position and average oxidation state.[s3] More theoretical calculations, such as density of state and Bader charge analysis, may need to be carried out to fully understand the valence state evolution of S in TiS_2 sodiation.

Comparison between MCR-ALS and Rietveld refinements:

A summary of quantification results of MCR-ALS and Rietveld refinements based on relative capacity (Table S2) and absolute capacity (Table S3) are shown below; because of the difference in the designs between the *operando* and *ex situ* analysis, changes were compared in terms of both relative and absolute capacity values.

The potential reasons why there is discrepancy among the two quantifying methods may be as the following. 1) The configurations of cell geometry in *operando* and *ex situ* measurements are different. Our *operando* cell is a tubing design which has a longer distance (2~6 mm) between anode and cathode. The longer distance provides the necessary to probe anode and cathode individually during the *operando* experiment but also leads to a longer diffusing path which results in the changes of kinetics during battery reaction. 2) The miniature cell design, while enables multiple cells to be measured consecutively during synchrotron experiment, where experimental efficiency needs to be carefully planned, also leads to several challenges; it was more challenging to acquire precise electrode weights as the amount of the coated slurry was less, and there may be a possibility of inhomogeneous reaction due to the cell geometry. These factors, while would not affect the analyses on phase identification reported in this work, they would contribute to the deviation of total capacity and corresponding *operando* analysis.

Table S2. Summary of quantification results of MCR-ALS and Rietveld refinements based on relative capacity.

		TiS_2	$Na_{0.55}TiS_2$	$NaTiS_2$
State 1 (40% relative capacity)	MCR-ALS	29%	66%	5%
	Rietveld refinements	10%	62%	20%
State 2 (82% relative capacity)	MCR-ALS	8%	37%	55%
	Rietveld refinements	0%	23%	76%

Table S3. Summary of quantification results of MCR-ALS and Rietveld refinements based on absolute capacity (mAh/g).

		TiS_2	$Na_{0.55}TiS_2$	$NaTiS_2$
State 1 (87 mAh/g)	MCR-ALS	16%	51%	20%
	Rietveld refinements	10%	62%	20%
State 2 (193 mAh/g)	MCR-ALS	0%	6%	94%
	Rietveld refinements	0%	23%	76%

References

s1. K. Sun, Q. Zhang, D. C. Bock, X. Tong, D. Su, A. C. Marschilok, K. J. Takeuchi, E. S. Takeuchi and H. Gan, *Journal of the Electrochemical Society*, 2017, **164**, A1291-A1297.

s2. L. Zhang, D. Sun, J. Kang, H. T. Wang, S. H. Hsieh, W. F. Pong, H. A. Bechtel, J. Feng, L. W. Wang, E. J. Cairns and J. H. Guo, *Nano Lett.*, 2018, **18**, 4506-4515.

s3. T. J. Pickering, R. C. Prince, T. Divers and G. N. George, *FEBS Lett.*, 1998, **441**, 11-14.